Copper Aluminate Spinel in the Stabilization and Detoxification of Simulated Copper-Laden Sludge

Yuanyuan Tang, Kaimin Shih*, King Chan

Department of Civil Engineering, The University of Hong Kong, Pokfulam Road, Hong Kong, Hong Kong SAR, China

* Corresponding author. Tel: +852-28591973; fax: +852-25595337.
E-mail address: kshih@hku.hk

Abstract

This study aims to evaluate the feasibility of stabilizing copper-laden sludge by the application of alumina-based ceramic products. The processing temperature, material leaching behaviour, and the effect of detoxification were investigated in detail. CuO was used to simulate the copper-laden sludge and X-ray Diffraction was performed to monitor the incorporation of copper into the copper aluminate spinel ($CuAl_2O_4$) phase in ceramic products. It was found that the development of $CuAl_2O_4$ increased with elevating temperatures up to and including 1000 ^oC in the 3 h short sintering scheme. When the sintering temperature went above 1000 ^oC, the $CuAl_2O_4$ phase began to decompose due to the high temperature transformation to $CuAlO_2$. The leachability and leaching behaviour of CuO and $CuAl_2O_4$ were compared by usage of a prolonged leaching test modified from U.S. EPA's toxicity characteristic leaching procedure. The leaching results show that $CuAl_2O_4$ is superior to CuO for the purpose of copper immobilization over longer leaching periods. Furthermore, the detoxification effect of $CuAl_2O_4$ was tested through bacterial adhesion with *Escherichia coli* K12, and the comparison of bacterial adhesion on CuO and $CuAl_2O_4$ surfaces shows the beneficial detoxification effect in connection with the formation of the $CuAl_2O_4$ spinel. This study demonstrates the feasibility of transforming copper-laden sludge into the spinel phase by using readily available and inexpensive ceramic materials, and achieving a successful reduction of metal mobility and toxicity.

Keywords: Sludge; Spinel; Ceramic; Stabilization; Detoxification; Copper

1. Introduction

The discharge of hazardous metals into receiving waters is detrimental to human health and the environment. As a type of hazardous metal that is subject to potential bioaccumulation, copper may cause stomach and intestinal distress, liver and kidney damage, and anaemia in humans (Gardea-Torresdey et al., 1996). Copper is present in the wastewater generated from printed circuit board manufacturing, electroplating, wire drawing, copper polishing, paint production, wood preservatives and printing operations. Common strategies that are chosen to remove hazardous metals from wastewater include physicochemical processes such as precipitation, coagulation, reduction, ion exchange and membrane processes (Park et al., 2005). However, the treatments mentioned above always result in the production of large amounts of hazardous-metal bearing sludge which requires additional treatment.

At present, sludge with hazardous metal residues needs to be disposed of in controlled landfills. However, the high cost of this strategy, combined with the limited number of landfills capable of accepting highly toxic metal wastes, has made the development of effective and economical treatment technologies essential. Many investigators have attempted to immobilize toxic metals using sorbents or cements and then correlating the performance directly with metal leachability (Kapoor and Viraraghavan, 1996; Lin et al., 1998; Bailey et al., 1999). However, solidification/stabilization technologies via sorption or cementation mechanisms are not generally successful in the prevention of leaching in acidic environments, i.e. a pH value less than 4.0 (Bonen and Sarkar, 1995; Yousuf et al., 1995).

Based on phase transformation at high temperature, attempts to stabilize radioactive waste in vitrified glass or ceramic materials have been carried out through a variety of thermal treatments (Lewis et al., 1993; Lewis et al., 1994; Wronkiewicz et al., 1997; Wang et al., 2005; Shih and Leckie, 2007). However, the products are not reusable due to their radioactive nature. A similar thermal treatment process with relatively lower firing temperatures (900-1600 ^{o}C) compared to vitrification may be helpful in promoting the effective incorporation of waste materials into ceramic products, such as bricks, tiles, refractories, and aggregates (Teixeira da Silva et al., 1998; Shih and Leckie, 2007). Converting hazardous sludge to ceramic products via well-controlled thermal treatment can remove hazardous metals from the waste stream and enable them to become reusable. The leachability of hazardous metals can be reduced because of the change of mineral phase after thermal treatment. Shih et al. (2006a, 2006b) successfully stabilized simulated nickel sludge by sintering with alumina, hematite and kaolinite as the ceramic raw materials. They reported significant reduction of nickel leachability from the spinel phases of the products, compared to the phase of nickel oxide.

It was previously reported that copper could be incorporated into the products sintered from clay materials, but the incorporation mechanism and phase transformation pathway have not been discussed in detail (Wei et al., 2001). An equilibrium phase diagram for Cu_2O-Al_2O_3 system was published (Wartenberg and Reuch, 1935), and the formation of the copper spinel was obtained by calcining the co-precipitation mixture of copper and aluminium hydroxide (Gadalla and White, 1964). Jacob and Alcock (1975) investigated the thermodynamics of copper aluminate spinel ($CuAl_2O_4$) formation and delineated the equilibrium phase diagram of the

86 Cu_2O-CuO-Al_2O_3 system. The above equilibrium studies have provided a great
87 opportunity to highlight the interaction between copper oxide and alumina at high
88 temperatures. It is thus anticipated that the incorporation of copper-laden sludge into
89 ceramic materials through thermal treatment may be a promising strategy for
90 stabilizing hazardous copper wastes. However, the potential of initiating copper spinel
91 formation in the industrial short-sintering scheme of ceramic products (i.e. tiles,
92 insulators, refractories) will require further investigation.
93
94 As an environmentally benign product, the material's surface should be capable of
95 supporting microbial activities. The adhesion of bacteria is usually the key factor for
96 developing biofilm on material surfaces, which later becomes the major support basis
97 for other biological growth. Due to the strong aquatic toxicity, copper oxide has been
98 used in paints for marine environments to reduce the formation of biofilm on material
99 surfaces. Copper-based paint may work as a selective medium for organisms by
100 creating a toxic boundary layer at the surface as the component biocides leach out
101 (Evans, 1981; Douglas-Helders et al., 2003). The use of copper-based paints to
102 prevent biofilm development and a biofouling effect has gained increasing attention
103 due to its environmental impact of releasing toxic copper ions into aquatic ecosystems
104 (Chamberlain et al., 1988; Katranitsas et al., 2003). It has been reported that concrete
105 sewer pipes coated with copper oxide exhibit antimicrobial characteristics and can
106 achieve 99% inhibition against the bacterium (Hewayde et al., 2007). Toxicities of
107 compounds can be measured singly and in mixtures of various complexities, using
108 acute toxicity bioassays (Fernández-Alba et al., 2001, 2002). Recently, Xu et al. (2005)
109 conducted a bacterium attachment study to evaluate the effectiveness of antifouling.
110 Therefore, the density of bacteria adhering to product's surfaces may potentially be

111 used to evaluate the results of metal detoxification after the incorporation of
112 hazardous copper waste into ceramics.
113
114 In this study, the effect of incorporating CuO, as the simulated copper-laden sludge,
115 into γ-alumina (γ-Al_2O_3) ceramic precursors was observed under a short sintering
116 process (3 h) with temperatures ranging 650-1150 ^oC. A prolonged leaching
117 procedure similar to the toxicity characteristic leaching procedure (TCLP) was carried
118 out to examine the stabilization effect of copper in the product phases. Whilst
119 considering the toxic nature of CuO for microbial adhesion, the surfaces of CuO and
120 the $CuAl_2O_4$ were compared through bacterial adhesion experiment to evaluate the
121 detoxification effect of producing the copper aluminate spinel in ceramics.
122
123
124 **2. Materials and Methods**
125
126 When thermally treated, the metal components of sludge are usually first
127 transformed into oxide forms and thus CuO (Sigma Aldrich) was used to simulate the
128 thermal reaction of copper-laden sludge. Experiments were carried out by firing the
129 mixture of CuO and γ-Al_2O_3 precursor. The γ-Al_2O_3 was prepared from HiQ-7223
130 alumina powder (Alcoa), which has a reported average particle size (d_{50}) of 54.8 nm.
131 The HiQ-7223 alumina was confirmed by X-ray Diffraction (XRD) to be the
132 boehmite phase (AlOOH; ICDD PDF # 74-1875), and after heat treatment at 650 ^oC
133 for 3 h it was successfully converted to γ-Al_2O_3 with an XRD crystallite size of 2-5
134 nm (Zhou and Snyder, 1991; Wang et al., 2005). The γ-Al_2O_3 precursor and CuO
135 were mixed to a total dry weight of 200 g at the Cu/Al molar ratio of 1:2, together

with 1 L of deionized water for ball milling of 18 h. The slurry samples were then dried and homogenized by mortar grinding. The derived powder was pressed into 20 mm pellets at 650 MPa to ensure consistent compaction of the powder sample in readiness for the sintering process. After sintering, the samples were air-quenched and ground into powder for XRD analysis and the leaching test.

Phase transformations during sintering were monitored by XRD. The diffraction patterns were collected using a Bruker D8 diffractometer (Bruker Co. Ltd.) equipped with Cu X-ray tube operated at 40 kV and 40 mA. Scans were collected from 10 to 90^{o} 2θ-angle, with a step size of 0.02^{o} and a counting time of 1 s $step^{-1}$. Phase identification was executed by matching XRD patterns with the powder diffraction files (PDF) database of the International Centre for Diffraction Data (ICDD). The leachability of the pure phase was tested using a leaching experiment which is a leaching procedure modified from the U.S. EPA SW-846 Method 1311 - Toxicity Characteristic Leaching Procedure (TCLP) with a pH 2.9 acetic acid solution (extraction fluid # 2) as the leaching fluid. Each leaching vial was filled with 10 mL of TCLP extraction fluid and 0.5 g of powder. The leaching vials were rotated end-over-end at 60 rpm for agitation periods of 0.75 to 22 d. At the end of each agitation period, the leachates were filtered with 0.2 μm syringe filters, the pH was measured and the concentrations of all metals were derived from ICP-AES (Perkin-Elmer Optima 3300 DV).

In this study, the bacterial adhesion experiment was carried out to first qualitatively observe the toxicity of $CuAl_2O_4$ surface. The *Escherichia coli* K12 bacteria strain was chosen for use in this adhesion evaluation on the surfaces of soda-lime glass (silica-

based), $CuAl_2O_4$ and CuO pellets. The culture solution was prepared with 10 g of peptone bacteriological (Beijing Chemical Works, 44075-2H, 250 g), 10 g of NaCl (Riedel-deHaen) and 5 g of yeast extract in 1 L of water. The glass material was taken from the microscope slides commonly designed for laboratory work, and it is an example of a non-toxic surface in the study of bacterial adhesion. The CuO powder was pressed into pellets and heated at 950 ^oC for 3 h. This was to effectively enhance the pellet strength and surface smoothness to facilitate the experimental needs, but also aimed to maintain the phase status (CuO) of the material. The mixture of CuO and γ-Al_2O_3 powder (Cu/Al molar ratio = 1:2) was also pressed into pellets and heated until $CuAl_2O_4$ was observed as the single phase in the product (990 ^oC for 20 d). Both CuO and $CuAl_2O_4$ pellets derived from the above processes were later polished by the diamond lapping films progressively down to a diamond grit size of 0.1 μm. Measurement of the surface roughness of glass, CuO and $CuAl_2O_4$ samples was conducted using a JPK Instruments atomic force microscope (AFM) equipped by silicon-cantilevers with a force constant of 0.1 N m^{-1} under the Cleveland method (Cleveland et al., 1993). Height images (40 × 40 μm^2) were used to calculate the roughness measurement based on the arithmetic average. Bacteria adhered on the substrata were stained with SYTO9 and observed using a fluorescence microscope (Nikon Eclipse E600).

3. Results and Discussion

3.1 Copper Spinel Formation

By sintering the mixture of CuO and γ-Al_2O_3, copper incorporation may proceed under a recrystallization reaction as follows:

$$CuO + \gamma\text{-}Al_2O_3 \rightarrow CuAl_2O_4 \quad (1)$$

It has been reported that the incorporation ability of γ-Al_2O_3 for nickel is affected by the sintering temperature (Shih et al., 2006a, 2006b). To investigate the effective temperature for alumina content to incorporate copper into the $CuAl_2O_4$ in the practice of sintering construction ceramic products, a 3 h short sintering scheme at temperatures ranging from 650 to 1150 ^oC was conducted. According to the database of the $CuAl_2O_4$ XRD pattern (ICDD PDF # 33-0448), its two major peaks are located at $2\theta = 36.868$ and 31.294^o, corresponding to the diffraction planes of (3 1 1) and (2 2 0) respectively. The result reveals that the sample sintered at 750 ^oC developed a distinguishable $CuAl_2O_4$ crystalline phase as shown in Fig. 1a. Jacob and Alcock (1975) observed the formation of the $CuAl_2O_4$ in their equilibrium thermal experiment (for 24 h) and reported the spinel formation temperature to start at 612 ^oC. However, when compared to the results observed in our short sintering experiment, it was discovered that an effective sintering period for industrial application to incorporate copper into $CuAl_2O_4$ in ceramic products should be at least above 750 ^oC. Since the solid state reaction is usually affected by both thermodynamic conditions and the diffusion process, this comparison may further suggest that spinel formation at temperatures below 750 ^oC is largely limited by the prevailing slow diffusion although it is thermodynamically feasible at temperatures above 612 ^oC. Below 750 ^oC, the $CuAl_2O_4$ phase formed by the short sintering scheme may only be limited at

210 the grain boundary of reactants, and the very small quantity of such phase in the
211 system was not reflected in the XRD results.
212
213 Two 2θ ranges of the XRD pattern (2θ = 36.4-37.4^{o} and 31.0-32.0^{o}) were selected
214 to further observe the peak intensity development to represent the $CuAl_2O_4$ spinel
215 product generated from the system at elevated temperatures (Fig. 2). Figure 2a
216 observes the crystallization of $CuAl_2O_4$ developed from the CuO + γ-Al_2O_3 precursor
217 within the 2θ range of 36.4-37.4^{o} at different sintering temperatures. Although there
218 was a distinguishable $CuAl_2O_4$ phase in the 750 ^{o}C sintered sample, the substantial
219 growth of $CuAl_2O_4$ in the system was observed to be at above 850 ^{o}C, which may
220 indicate the energy needed to overcome the major diffusion barrier in the system.
221 Below 1000 ^{o}C, the peak intensity of the $CuAl_2O_4$ phase increases as the temperature
222 increases. However, at sintering temperatures higher than 1000 ^{o}C, the peak intensity
223 of the $CuAl_2O_4$ phase was found to decrease with elevated temperatures.
224
225 The XRD patterns within the 2θ range of 31.0-32.0^{o} (Fig. 2b) show that the
226 decrease of $CuAl_2O_4$ at higher temperatures was due to the formation of another new
227 Cu-Al oxide phase, cuprous aluminate delafossite ($CuAlO_2$; ICDD PDF # 75-2356).
228 Figure 2b has further verified the optimal formation temperature of $CuAl_2O_4$ at 1000
229 ^{o}C, and the phase transformation to $CuAlO_2$ at higher temperatures was observed by
230 the (0 0 6) diffraction plane signal of $CuAlO_2$ at 2θ around 31.63^{o}. Since the decrease
231 of $CuAl_2O_4$ at higher temperatures was accompanied with a corresponding increase of
232 $CuAlO_2$ in the system, it is suggested that the formation of $CuAlO_2$ occurred
233 immediately after the decomposition of $CuAl_2O_4$, or went through structural
234 transformation by discharging the excessive aluminum and oxygen from the crystal

structure. Nevertheless, both phase transformation mechanisms indicate that the opportunity of immobilizing copper from the Al-O incorporated structures is small when this phase transformation process takes place at high temperatures. Together with the interaction between unreacted CuO and Al_2O_3 (Jacob and Alcock, 1975), the $CuAlO_2$ formation mechanisms at temperatures above 1000 ^oC can be organized in the following way:

$$2CuAl_2O_4 \rightarrow 2CuAlO_2 + Al_2O_3 + 0.5O_2 \quad (2)$$

$$2CuO \rightarrow Cu_2O + 0.5O_2 \quad (3)$$

$$Cu_2O + Al_2O_3 \rightarrow 2CuAlO_2 \quad (4)$$

3.2 The Leaching Mechanisms

To investigate the effect of copper immobilization after the incorporation by the spinel structure, the preferred method was to first compare the leachability of single phase samples under the same leaching environment. Therefore, this study prepared a leaching experiment sample with $CuAl_2O_4$ as the only phase appearing in the sample. From the incorporation efficiency experiment, it was observed that 1000 ^oC as the sintering temperature could attain the highest yield of $CuAl_2O_4$ phase without initiating the formation of the $CuAlO_2$ phase, although small amounts of reactants (Al_2O_3 and CuO) were still observed in the system. To ensure the complete transformation of reactants to the product phase ($CuAl_2O_4$), a longer sintering time (20 d) was used to facilitate reaction equilibrium. Moreover, the sintering temperature of 990 ^oC, which is slightly less than 1000 ^oC, was chosen to further prevent the generation of the $CuAlO_2$ phase during the prolonged sintering process. The XRD

pattern in Fig. 1b shows the success achieved by preparing the $CuAl_2O_4$ sample, where no peak of CuO or Al_2O_3 reactant phase was found in the pattern.

Samples used in the leaching test were ground into powder and measured to ascertain the BET surface area to yield values of 1.35 $m^2 g^{-1}$ for $CuAl_2O_4$ and 0.17 $m^2 g^{-1}$ for CuO. The pH values are shown in Fig. 3a, which reveals the greater pH increase of CuO leachate. Within the first few days, the pH of CuO leachate experienced a significant increase which was then maintained at around 4.7-4.9 throughout the rest of the leaching period. In contrast, the pH of the $CuAl_2O_4$ leachate was maintained at the beginning value of its leaching fluid throughout the entire leaching period. The increase of leachate pH may arise due to the dissolution of cations through ion exchange with protons in the solution. This is accompanied by the destruction of crystals at the solid surface by the acidic leaching fluid. The increase in leachate pH may indicate that CuO is more vulnerable to proton-mediated dissolution. On the other hand, $CuAl_2O_4$ (sintered from γ-Al_2O_3 + CuO) may show higher intrinsic resistance to such acidic attack, even with higher surface areas.

As the leaching for solid is likely dominated by surface reactions, it is expected to be proportional to sample surface area. In addition, since the same weight of sample (0.5 g) was always used, the total copper content in the sample, subject to the different copper phases, should also be normalized for comparison. Figure 4 summarizes the amounts of leached copper from samples normalized with respect to the surface areas of tested solids. The copper in the CuO leachate was over 400 times higher than that in the $CuAl_2O_4$ leachate near the end of the leaching period. This confirms that the $CuAl_2O_4$ spinel phase has a higher intrinsic resistance to such acidic attack compared

285 to the CuO phase and the sintering strategy designed for copper-laden sludge is
286 proven to be beneficial in stabilizing copper. The curve in the small diagram of Fig. 4
287 further provides the details of copper concentrations in the $CuAl_2O_4$ leachate.
288
289 When the pH of the CuO leachate reached ~ 4.9, the leaching of CuO stabilized at a
290 copper concentration of ~ 2500 mg L^{-1} (~ $10^{-1.4}$ M) in the leachate. As a general
291 assumption of cation-proton exchange mechanism, the destruction of copper oxide by
292 the acidic attack of the solution can be expressed as:
293
294 $$CuO_{(s)} + 2H^{+}_{(aq)} \rightarrow Cu^{2+}_{(aq)} + H_2O \quad (5)$$
295
296 However, the concentration of copper ions in the solution [$Cu^{2+}_{(aq)}$] is also limited
297 by the potential precipitation/dissolution reactions, such as in respect to $Cu(OH)_{2(s)}$:
298
299 $$Cu(OH)_{2(s)} \leftrightarrow Cu^{2+}_{(aq)} + 2OH^{-}_{(aq)} \quad (6)$$
300
301 where the solubility constant (K_{sp}) of Eq. 6 is $10^{-19.25}$ (Stumm and Morgan, 1996). At
302 pH 4.9, the product of [$Cu^{2+}_{(aq)}$] × [$OH^{-}_{(aq)}$]^2 was found to be $10^{-19.6}$, which is very
303 close to the K_{sp} of $Cu(OH)_{2(s)}$. This result indicates that the system was very close to
304 the saturation of $Cu(OH)_{2(s)}$ and the stabilization of copper concentration in the CuO
305 leachate was likely controlled through the equilibrium with the $Cu(OH)_{2(s)}$ phase.
306
307 When leaching the $CuAl_2O_4$ phase, a "congruent dissolution" through the cation-
308 proton exchange reaction can be written as:
309

$$CuAl_2O_{4(s)} + 8H^+_{(aq)} \rightarrow Cu^{2+}_{(aq)} + 2Al^{3+}_{(aq)} + 4H_2O \quad (7)$$

Such congruent dissolution would result in a theoretical $[Al^{3+}_{(aq)}]/[Cu^{2+}_{(aq)}]$ molar ratio of 2.0 in the leachates. However, this ratio was observed at 0.75-0.80 in the leachate of $CuAl_2O_4$ as shown in Fig. 3b. Since the system was maintained in a more acidic environment (~ pH 3.2) and the copper concentration was much lower than that of the CuO leachate, the copper concentrations in the leachates of $CuAl_2O_4$ were all considerably under-saturated regarding to the $Cu(OH)_{2(s)}$ phase. The aluminium concentrations measured in the $CuAl_2O_4$ leachates were ~ 9.5 mg L^{-1} (~ $10^{-3.45}$ M). The reaction of amorphous aluminium hydroxide precipitation/dissolution is:

$$am{\bullet}Al(OH)_{3(s)} \leftrightarrow Al^{3+}_{(aq)} + 3OH^-_{(aq)} \quad (8)$$

where the solubility constant (K_{sp}) of Eq. 8 is $10^{-32.7}$ (Stumm and Morgan, 1996). The product of $[Al^{3+}_{(aq)}] \times [OH^-_{(aq)}]^3$ was found to be $10^{-35.9}$ and it did not reach the saturation ($[Al^{3+}_{(aq)}] \times [OH^-_{(aq)}]^3 = 10^{-32.7}$) of amorphous $Al(OH)_{3(s)}$ either. Therefore, this suggests that the leaching behaviour of $CuAl_2O_4$ in this experiment is likely to be an incongruent dissolution, where the majority of the Al-O bonds still remained on the $CuAl_2O_4$ spinel surface. Although some previous studies (Cailleteau et al., 2008; Ohlin et al., 2010) have further suggested the reorganization of remaining molecules in incongruent dissolution scenarios, the overall result indicates the existence of an Al-rich layer on the leached $CuAl_2O_4$ surface, which is beneficial for preventing the further leaching of Cu and may increase product durability.

3.3 Adhesion of *E. coli*

335

336 Since the density of bacteria adhering to the product surface may potentially be
337 used to evaluate the results of metal detoxification, this study first conducted a
338 qualitative comparison of bacterial adhesion on the substrata of the $CuAl_2O_4$ spinel,
339 CuO and soda-lime (silica-based) glass. Experimental studies have suggested the
340 importance of the physicochemical and thermodynamic properties of both the
341 substrata and the bacterial cell surface during the process of bacterial adhesion (Van
342 Loosdrecht et al., 1989; Sjollema et al., 1990; Vadillo-Rodriguez and Logan, 2006).
343 In this study, a type of testing bacteria, *E. coli* K12, was cultivated in a solution with a
344 pH of ~ 6.5 and all the substratum samples were collectively placed in the same
345 solution for better comparison. Since surface roughness may impact bacterial
346 adhesion (Brant and Childress, 2002), the tested surfaces of samples were polished
347 using diamond lapping films and the roughness values were measured by AFM to be
348 2.3±1.7, 491±192 and 369±90 nm for glass, $CuAl_2O_4$ and CuO, respectively.
349

350 Figure 5 shows the results from the comparison of *E. coli* bacterial adhesion on the
351 surface of glass, $CuAl_2O_4$ and CuO after 18 h of bacterial cultivation. The amount of
352 *E. coli* adhering to the glass surface visibly surpassed the amount on the surfaces of
353 both the $CuAl_2O_4$ and CuO samples (Fig. 5a). However, due to the toxicity effect, no
354 bacterial adhesion was found on the surface of the CuO substratum as shown in the
355 Fig. 5c. With much lower copper leachability as compared to CuO, the $CuAl_2O_4$
356 spinel clearly developed bacterial adhesion on the surface which showed its capacity
357 to support microbial activities, although the level was lower than that of the glass
358 substratum (Fig. 5b).
359

As the inhibition effect of copper oxide on biofouling has already been indicated (Evans, 1981; Balls, 1987; Chamberlain et al., 1988; Hodson and Burke, 1994; Douglas-Helders et al., 2003; Katranitsas et al., 2003; Hewayde et al., 2007), the comparison result of glass and CuO in this study is consistent with previous findings. Moreover, some studies suggested that the increase of nano-scale roughness of a surface increases bacterial adhesion (Shellenberger and Logan, 2002); other studies have demonstrated no significant relationship between surface roughness and bacterial adhesion (Li and Logan, 2004). In our work, the highest level of bacteria adhered to the glass surface, even with much lower roughness, thus indicating the dominant effect of substrata material. The growth of bacteria on the surface of the $CuAl_2O_4$ substratum suggests the successful detoxification of copper through the stabilization strategy of incorporating CuO into the aluminate spinel phase. Since the formation of a biofilm covering on a surface begins with the adhesion of a small number of bacteria, the results shown here provide direct evidence of the environmental friendliness of waste-incorporated ceramic products. Such information on the intrinsic properties of material is also important and beneficial when aiming to minimize the environmental impact even after the end of a product's life.

Acknowledgements

We acknowledge the funding for this research provided by the University of Hong Kong from its Research Seed Fund. The authors are thankful to Professor Xiang-Dong Li for providing the ICP-AES analysis. Dr. Tong Zhang, Mr. Yuanqing Chao and Ms.

Vicky Fung are thanked for assisting with the AFM technique and bacterial adhesion experiment.

References

Bailey, S.E., Olin, T.J., Bricka, R.M., Adrian, D.D., 1999. A review of potentially low-cost sorbents for heavy metals. Water Res. 33 , 2469-2479.

Balls, P.W., 1987. Tributylin (TBT) in the waters of a Scottish Sea Loch arising from the use of antifoulant treated netting by salmon farms. Aquaculture 65, 227-237.

Bonen, D., Sarkar, S.L., 1995. The effect of simulated environmental attack on immobilization of heavy metal doped in cement-based materials. J. Hazard. Mater. 40, 321-335.

Brant, J.A., Childress, A.E., 2002. Assessing short-range membrane-colloid interactions using surface energetics. J. Membrane Sci. 203, 257-273.

Cailleteau, C., Angeli, F., Devreux, F., Gin, S., Jestin, J., Jollivet, P., Spalla, O., 2008. Insight into silicate-glass corrosion mechanisms. Nat. Mater. 7, 978-983.

Chamberlain, A.H.L., Simmonds, S.E., Garner, B.J., 1988. Marine 'copper-tolerant' sulphate reducing bacteria and their effects on 90/10 copper-nickel (CA 706). Int. Biodeterior. 24, 213-219.

Cleveland, J.A., Manne, S., Bocek, D., Hansma, P.K., 1993. A nondestructive method for determining the spring constant of cantilevers for scanning force microscopy. Rev. Sci. Instrum. 64, 403-405.

Douglas-Helders, G.M., Tana, C., Carson, J., Nowak, B.F., 2003. Effects of copper-based antifouling treatment on the presence of *Neoparamoeba pemaquidensis* Page, 1987 on nets and gills of reared Atlantic salmon (*Salmo salar*). Aquaculture 221, 13-22.

Evans, L.V., 1981. Marine algae and fouling-a review, with particular reference to ship-fouling. Bot. Mar. 24, 167-171.

Fernández-Alba, A.R., Hernando, M.D., López, G.D., Chisti, Y., 2001. Toxicity of pesticides in wastewater: a comparative assessment of rapid bioassays. Anal. Chim. Acta 426, 289-301.

Fernández-Alba, A.R., Hernando, M.D., López, G.D., Chisti, Y., 2002. Toxicity evaluation of single and mixed antifouling biocides measured with acute toxicity bioassays. Anal. Chim. Acta 456, 303-312.

Gadalla, A.M.M., White, J., 1964. Equilibrium relationships in the system CuO-Cu_2O-Al_2O_3. J. Brit. Ceram. Soc. 63, 39-62.

Gardea-Torresdey, J.L., Tang, L., Salvador, J.M., 1996. Copper adsorption by esterified and unesterified fractions of Sphagnum peat moss and its different humic substances. J. Hazard. Mater. 48, 191-206.

Hewayde, H., Nakhla, G.F., Allouche, E.N., Mohan, P.K., 2007. Beneficial impact of coatings on biological generation of sulphide in concrete sewer pipes. Struct. Infrastruct. E. 3, 267-277.

Hodson, S.L., Burke, C., 1994. Microfouling of salmon-cage netting: a preliminary investigation. Biofouling 8, 93-105.

Jacob, K.T., Alcock, C.B., 1975. Thermodynamics of $CuAlO_2$ and $CuAl_2O_4$ and Phase equilibria in the system Cu_2O-CuO-Al_2O_3. J. Am. Ceram. Soc. 58, 192-195.

Kapoor, A., Viraraghavan, T., 1996. Discussion: Treatment of metal industrial wastewater by fly ash and cement fixation. J. Environ. Eng.-ASCE. 122, 243-244.

Katranitsas, A., Castritsi-Catharios, J., Persoone, G., 2003. The effects of a copper-based antifouling paint on mortality and enzymatic activity of a non-target marine organism. Mar. Pollut. Bull. 46, 1491-1494.

Lewis, M.A., Fischer, D.F., Murphy, C.D., 1994. Properties of glassbonded zeolite monlith. Ceram. Trans. 45, 277-286.

Lewis, M.A., Fischer, D.F., Smith, L.J., 1993. Salt-occluded zeolite as an immobilization matrix for chloride waste salt. J. Am. Ceram. Soc. 76, 2826-2832.

Li, B., Logan, B.E., 2004. Bacterial adhesion to glass and metal-oxide surfaces. Colloid. Surface B. 36, 81-90.

Lin, C.F., Lo, S.S., Lin, H.Y., Lee, Y., 1998. Stabilization of cadmium contaminated soils using synthesized zeolite. J. Hazard. Mater. 60, 217-226.

Ohlin, C.A., Villa, E.M., Rustad, J.R., Casey, W.H., 2010. Dissolution of insulating oxide materials at the molecular scale. Nat. Mater. 9, 11-19.

Park, D., Lee, D.S., Park, J.M., Chun, H.D., Park, S.K., Jitsuhara, I., Miki, O., Kato, T., 2005. Metal recovery from electroplating wastewater using acidophilic iron oxidizing bacteria: Pilot-scale feasibility test. Ind. Eng. Chem. Res. 44, 1854-1859.

Shellenberger, K., Logan, B.E., 2002. Effect of molecular scale roughness of glass beads on colloidal and bacterial deposition. Environ. Sci. Technol. 36,184-189.

Shih, K., Leckie, J.O., 2007. Nickel aluminate spinel formation during sintering of simulated Ni-laden sludge and kaolinite. J. Eur. Ceram. Soc. 27, 91-99.

Shih, K., White, T., Leckie, J.O., 2006a., Spinel formation for stabilizing simulated nickel-laden sludge with aluminum-rich ceramic precursors. Environ. Sci. Technol. 40, 5077-5083.

Shih, K., White, T., Leckie, J.O., 2006b. Nickel stabilization efficiency of aluminate and ferrite spinels and their leaching behavior. Environ. Sci. Technol. 40, 5520-5526.

Sjollema, J., van der Mei, H.C., Uyen, H.M.W., Busscher, H.J., 1990. The influence of collector and bacterial cell surface properties on the deposition of oral streptococci in a parallel plate flow cell. J. Adhes. Sci. Technol. 4, 765-779.

Stumm, W., Morgan, J.J., 1996. Aquatic Chemistry. 3rd Ed. Wiley Interscience, New York.

Taboada-Serrano, P., Vithayaveroj, V., Yiacoumi, S., Tsouris, C., 2005. Surface charge heterogeneities measured by atomic force microscopy. Environ. Sci. Technol. 39, 6352-6360.

Teixeira da Silva, V.L.S., Lima, F.P., Dieguez, L.C., Schmal, M., 1998. Regeneration of a deactivated hydrotreating catalyst. Ind. Eng. Chem. Res. 37, 882-886.

Vadillo-Rodriguez, V., Logan, B.E., 2006. Localized attraction correlates with bacterial adhesion to glass and metal oxide substrata. Environ. Sci. Technol. 40, 2983-2988.

Van Loosdrecht, M.C.M., Lyklema, L., Norde, L., Zehnder, A.J.B., 1989. Bacterial adhesion: a physicochemical approach. Microb. Ecol. 17, 1-15.

Wang, Y., Suryanarayana, C., An, L., 2005. Phase transformation in nanometer-sized γ-alumina by mechanical milling. J. Am. Ceram. Soc. 88, 780-783.

Wartenberg, H., von Reusch, H.J., 1935. Melting diagram of refractory oxides: IV. Z. Anorg. Allg. Chem. 207, 1-20.

Wei, Y.L., Yang, Y.W., Cheng, N., 2001. Study of thermally immobilized Cu in analogue minerals of contaminated soils. Environ. Sci. Technol. 35, 416-421.

Wronkiewicz, D.J., Bates, J.K., Buck, E.C., Hoh, J.C., Emery, J.W., Wang, L.M., 1997. Radiation Effects in Moist-air Systems and the Influence of Radiolytic Product Formation on Nuclear Waste Glass Corrosion. Argonne National Laboratory Report No. ANL-97/15, Argonne.

Xu, Q.W., Barrios, C.A., Cutright, T., Newby, B.Z., 2005. Evaluation of toxicity of capsaicin and zosteric acid and their potential application as antifoulants. Environ. Toxicol. 20, 467-474.

Yousuf, M., Mollah, A., Vempati, R., Lin, T., Cocke, D., 1995. The interfacial chemistry of solidification/stabilization of metals in cement and pozzolanic material systems. Waste Manage. 15, 137-148.

Zhou, R.S., Snyder, R.L., 1991. Structures and transformation mechanisms of the η, γ and θ transition aluminas. Acta Crystallogr. B 47, 617-630.

Fig. 1. The XRD pattern of the CuO + γ-Al_2O_3 system shows the formation of the copper aluminate spinel when sintering at (a) 750 ^oC for 3 h, and (b) 990 ^oC for 20 d. The "C" represents copper oxide (CuO, ICDD PDF # 48-1548) and the "S" is for the copper aluminate spinel ($CuAl_2O_4$, ICDD PDF # 33-0448). The XRD pattern in (b) shows that $CuAl_2O_4$ was the only phase in the sample and it was later used to test the $CuAl_2O_4$ leachability.

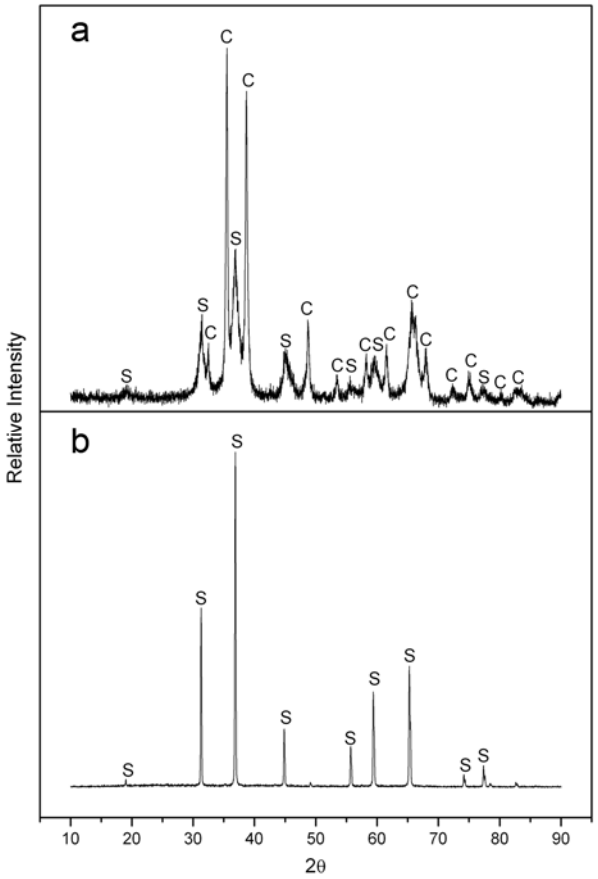

Fig. 2. The comparison of XRD patterns between (a) 2θ = 36.4° and 37.4° (b) 2θ = 31.0° and 32.0° for CuO + γ-Al_2O_3 samples (with a molar ratio for Cu:Al of 1:2) sintered at 650 - 1150 °C for 3 h. The formation of $CuAl_2O_4$ was found to reach its maximum at 1000 °C, and the curves at the top-right corners of (a) and (b) illustrate the relative intensities of the spinel peaks at 2θ = 36.868° and 2θ = 31.294°, respectively. The phase transformation to $CuAlO_2$ at higher temperatures was observed by the peak at 2θ around 31.63°.

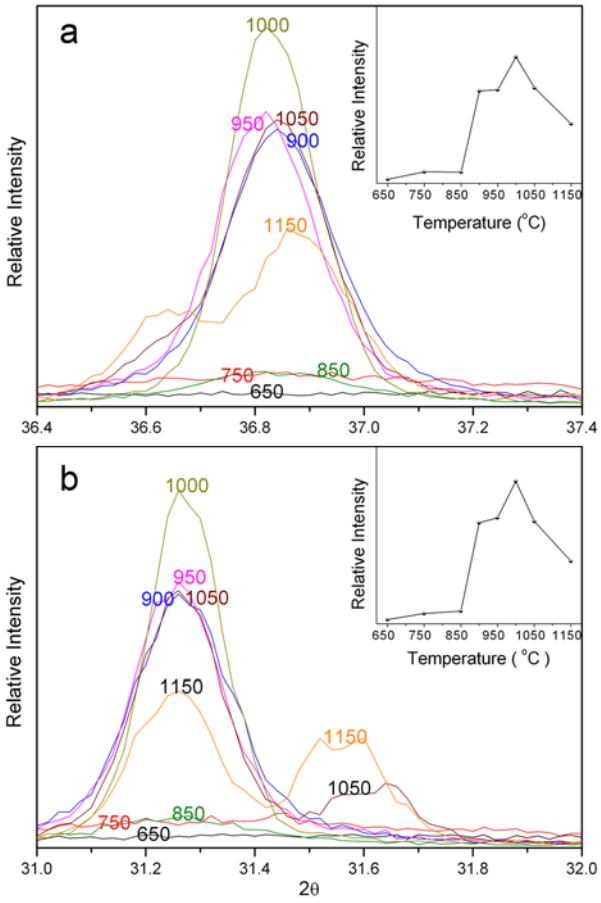

Fig. 3. The (a) pH values and (b) [Al]/[Cu] molar ratios of the leachates of the CuO and $CuAl_2O_4$ phases. The leaching solution was TCLP extraction fluid no. 2 (acetic acid solution) with a pH of 2.9. Each leaching vial was filled with 10 ml of extraction fluid and 0.5 g of powder sample, and then rotated end-over-end between 0.75 and 22 d.

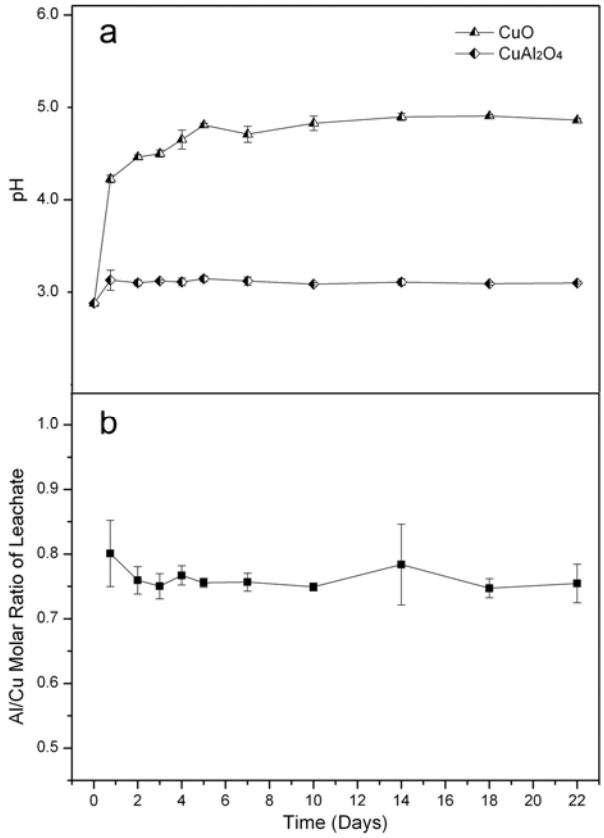

Fig. 4. Normalized copper concentrations in the leachates of CuO and $CuAl_2O_4$. The surface area of CuO powder is 0.17 m^2 g^{-1} and the surface area of $CuAl_2O_4$ is 1.35 m^2 g^{-1}. The leaching solution was TCLP extraction fluid no. 2 (acetic acid solution) with a pH of 2.9. Each leaching vial was filled with 10 ml of extraction fluid and 0.5 g of powder samples, and then rotated end-over-end between 0.75 and 22 d. The curve in the small diagram further provides the details concerning the copper concentrations in the $CuAl_2O_4$ leachate.

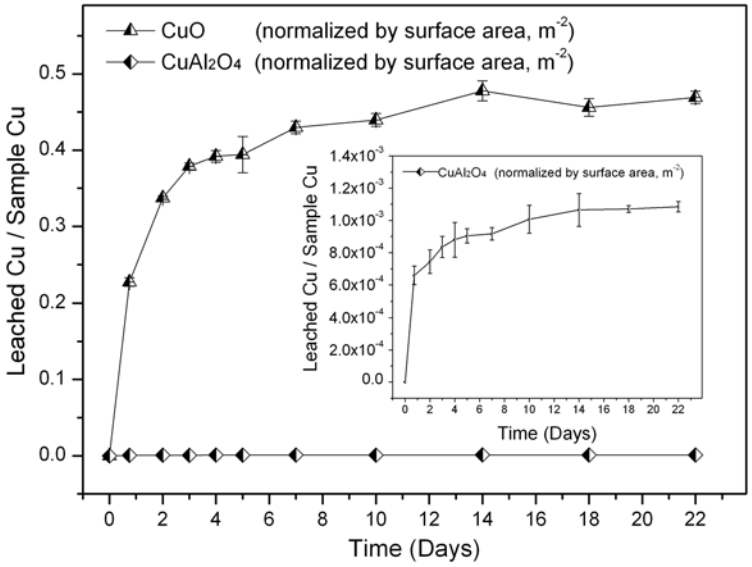

Fig. 5. The *Escherichia coli* K12 bacterial adhesion on the surface of (a) glass, (b) $CuAl_2O_4$ and (c) CuO. All three materials were used as substrate and cultured for 18 h in the same solution containing *E. coli* K12 bacteria.